ISSN: 0067-2904

Natural Attenuation Modelling of Heavy-Metal in Groundwater of Kirkuk City, Iraq

Jawdat Abdul Jalil M. Zaki Al-Hamdani[1], Habil Broder J. Merkel[2], Salih Muhammad Awadh[3]*, Omer Sabah Ibrahiem[4]

[1]General Commission for Groundwater, Ministry of Water Resources, Iraq
[2]Department of Hydrogeology, Institute for Geology, TU Bergakademie Freiberg, Germany
[3]Department of Geology, College of Science, University of Baghdad, Iraq
[4]Environmental Research Unit, College of Science, Kirkuk University, Iraq

Abstract

This study deals with the shallow alluvial aquifer situated beneath the urban area of kirkuk city. The ancient part of the city (Shorja) is affected by seepage from local agricultural areas causing relatively high heavy metals concentration in groundwater. The selection of polluted site depended on the highest TDS value (3856 mg/L) associated with the highest heavy metal concentrations (Pb, Ni, Co and Zn) in groundwater. This study focuses on the evaluation of natural attenuation effectivity for long-term protection of groundwater quality using realistic three-dimensional reactive-transport groundwater model. The requirements of 3-dimensional reactive transport model were obtained from field observation and laboratory works, in addition to aquifer stratigraphy, minerology and hydrochemistry. The simulations were achieved by using PHAST program that is depended on the HST3D flow and transport code and the hydrochemical PHREEQC code. The modeling results explained the ability of natural attenuation in consuming the concentration of heavy metals, where Long-term (20 year) simulation results show that heavy metal adsorption on hydrous ferric oxide, effectively capture the movement of heavy metals in groundwater down gradient of source areas, resulting in an basically immobile groundwater plume.

Keywords: Groundwater; Heavy metals; Natural attenuation; Reactive transport modeling; PHREEQC; PHAST.

موديل التوهين الطبيعي للمعادن الثقيلة في المياه الجوفية لمدينة كركوك، العراق

جودت عبد الجليل محمد زكي الحمداني[1]، هابل برودر جي ميركل[2]، صالح محمد عوض[3]*، عمر صباح ابراهيم[4]

[1]الهيئة العامة للمياه الجوفية، ووزارة الموارد المائية، العراق
[2]قسم جيولوجيا المياه، معهد الجيولوجيا، جامعة فرايبرغ، ألمانيا
[3]قسم الجيولوجيا، كلية العلوم، جامعة بغداد، العراق
[4]وحدة البحوث البيئية، كلية العلوم، جامعة كركوك، العراق

الخلاصة:

يوجد خزان المياه الجوفية الغريني الضحل أسفل المنطقة الحضرية في مدينة كركوك. يتأثر الجزء القديم من المدينة (الشورجة) بالتسرب من المنطقة الزراعية المحلية مما يجعل تراكيز المعادن الثقيلة في المياه الجوفية مرتفعة نسبيا. تم تحديد الموقع الملوث استناداً إلى اعلى قيمة للأملاح الصلبة الكلية (3856 ملغ/لتر) والمصاحب لأعلى تركيز للمعادن الثقيلة (الرصاص، النيكل، الكوبلت والزنك) في المياه الجوفية. تركز هذه الدراسة على تقييم فعالية التوهين الطبيعية على المدى الطويل لحماية نوعية المياه الجوفية باستخدام موديل

*Email: salihauad2000@yahoo.com

واقعي ثلاثي الأبعاد لتفاعل النقل للمياه الجوفية. تم الحصول على متطلبات موديل تفاعل النقل ثلاثي الأبعاد من المراقبة الميدانية والاعمال المختبرية، بالإضافة إلى دراسة الخصائص الطباقية والمعدنية والهايدروكيميائية لطبقة المياه الجوفية،. تم إجراء المحاكاة باستخدام برنامج PHAST والذي يعتمد على برنامج تفاعل النقل والتدفق HST3D وبرنامج PHREEQC الهيدروكيميائي. أوضحت نتائج الموديل قدرة التوهين الطبيعي في استهلاك تراكيز المعادن الثقيلة، حيث اظهرت نتائج المحاكاة طويلة الامد (20 سنة) أن امتزاز المعادن الثقيلة على أكاسيد الحديد المائية تعيق حركة المعادن الثقيلة على نحو فعال في المياه الجوفية أسفل الميل من منطقة المصدر، مما يؤدي بصورة اساسية الى الحد من حركة الجسم الملوث في المياه الجوفية.

Introduction

Hydrogeochemical characterization of shallow groundwater in the urban areas reflects the level of contamination that occurred by many sources such as the infiltration of storm water, the leakage of wastewater, and industrial activities [1-5]. The influence of heavy metals from anthropogenic pollution on the quality of urban groundwater is not clear, due to underground heterogeneity and the large variability in different controlling parameters such as soil composition, grain-size distribution, and hydraulic properties [6-12]. The main source of heavy metals in Kirkuk area was emissions from oil trash burning, vehicle exhaust and industrial activities [13-16]. Moreover, the population of Kirkuk city is predicted to increase from 1,050,000 in 2008 to 1,445,556 in 2020, which contribute to increase the quantity and size of Municipal solid waste. The expected waste may reach up to 1000 tone in 2011. By 2021, the daily waste may amount to 1200 tones, which poses a serious problem having adverse effects on environment and health of the citizens [17]. On the other hand, the gradual growth of the urban area may effect on groundwater quality by reducing the water well protection zones and consequently results in pollution of pumping wells [18]. This study focuses on mechanistic approach to modeling heavy metal sorption behavior using thermodynamic principles, because it is more active and widely used in combined effects the variations of ionic strength and pH within the aquifer in the model [19]. For this purpose, PHAST code was used. It is based on the solute transport model HST3D and contains the same reactions existing in PHREEQC code including mineral equilibrium, water-gas equilibrium, cation exchange, surface complexation, solid solutions, and kinetic reactions [20-24]. The HST3D code is suitable for simulating groundwater in saturated three-dimensional flow systems with mutable density and viscosity [20, 21]. Chemical sorption of metals in groundwater occurs due to chemical bond between the molecule of the solute and the adsorbent. The adsorbed molecules are restricted at specific sites in solid phase and therefore are not free to migrate on the surface. Chemical adsorption is generally irreversible and exothermic [25] in the specified pH and Eh values. The sorption processes prevent metal mobility in most natural aqueous systems [26, 27], whereas the total amount of metals in an aquifer remains the same. Metals can only change their form to be immobilized in solid phase [28]. The objective of this research is to determine the special distribution of dissolved, adsorbed, and solid phase heavy metal concentration in groundwater beneath Kirkuk city by building a reactive transport model to test an in-situ natural attenuation.

Regional setting of the study area

The urban area of Kirkuk city is located 250 km north of Baghdad between latitudes 35˚ 30.162' – 35˚ 30.195' N and longitude 44˚ 26.304' – 44˚ 26.259' E, spreading over an area of approximately 100 km² (Figure 1). Elevation of the study area ranges between 329 meter above sea level (m.a.s.l.), with the highest elevation 374 m.a.s.l. in the northeastern part and the lowest elevation 294 m.a.s.l. in the southwestern part. The Khassa River is the main and only hydrologic feature in the region, which is ephemeral river flowing from northeast to southwest with length of 14 Km within study area. This river cuts across the central of Kirkuk city, and it joins the main tributary of the Tigris River. The study area is characterized by a humid subtropical climate [29], almost dry, hot dry in summer and cold rainy in winter. Long-term monthly mean rainfall, temperature, relative humidity, and potential evapotranspiration are 600 mm/month, 20 °C, 46%, and 1500 mm/month, respectively.

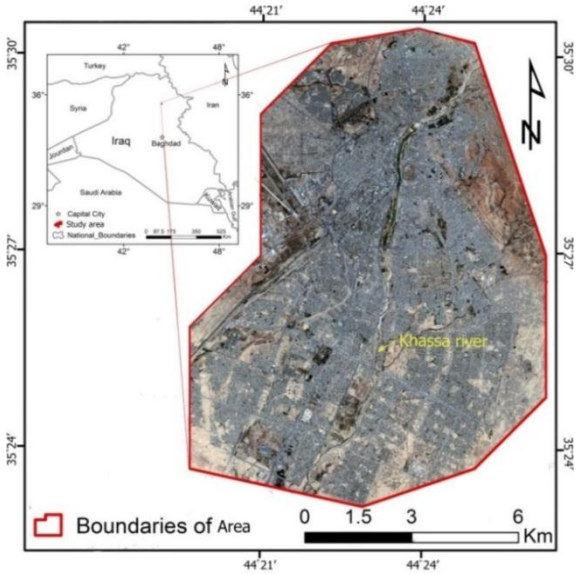

Figure 1- location map of the study area

Stratigraphically, Fatha (M. Miocene), Injana (U. Miocene) and Al-Mukdadyia (L. Pliocene) formations are exposed in the northeastern part of study area [30]. Alluvial Quaternary deposits as a sheet run-off and slope deposits cover the remaining flat areas between Kirkuk and Jambur anticlines Figure-2. Alluvial deposits are formed by the deposition and erosion during different stages of river flooding is commonly consisted of clayey silt, sand and gravel with secondary gypsum (gypcrete) [31-34].

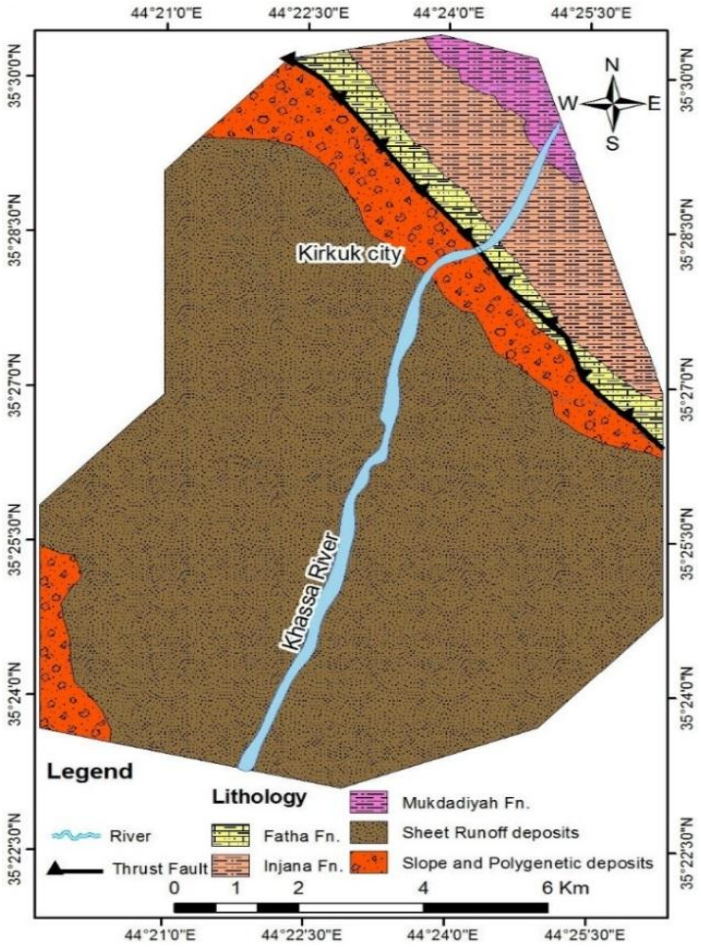

Figure 2- Geological map of study area

Materials And Methods

Sampling and Analysis

Forty-six wells in the study area were studied. Twenty-five boreholes with total depth exceed 100m through Quaternary deposits were studied individually depending on their lithological description to determine aquifer properties and to create fence diagram and aquifer model using RockWorks16 program Figure-3. The remaining wells were used for monitoring the fluctuation of water table and determining the chemistry of groundwater. Groundwater samples were collected systematically as one sample per 2 km^2 to get a uniform coverage of the study area [35] Figure-4, in which twenty five water samples were collected at 21 locations for each high and low water season in April and September 2014 respectively. The coordinates (Latitude, Longitude and elevation) for each well was determined using GPS instrument (Garmin etrex vista). The wells were coded from GW-1 to GW-21. Water table was measured at each well using sounder instrument before sampling. Physical properties of groundwater samples were measured in the field, such as pH, temperature, electrical conductivity (µS/ cm) and dissolved oxygen (mg/L), using portable devices (WTW pH 3110/Temperature, HM ORP-200, WTW Cond 3110, WP 600 Series oxygen Meters) after calibrated with standard solutions. Three bottles were taken from each site for analyzing major ions, minor ions and Trace element. Samples of the major ions were transported in a cooled box at 4°C (with ice packs) to analysis in the Laboratory of the General Commission of Groundwater. Heavy metal samples were decanted into 100 cm3 polyethylene bottles and directly acidified to pH<2 by adding a few drops of ultra-pure nitric acid. Concentrations of heavy metal were measured by an inductively coupled plasma mass spectrometer, ICP-MS (Thermo X-Series II) in Water chemistry laboratory of TU Bergakademie Freiberg.

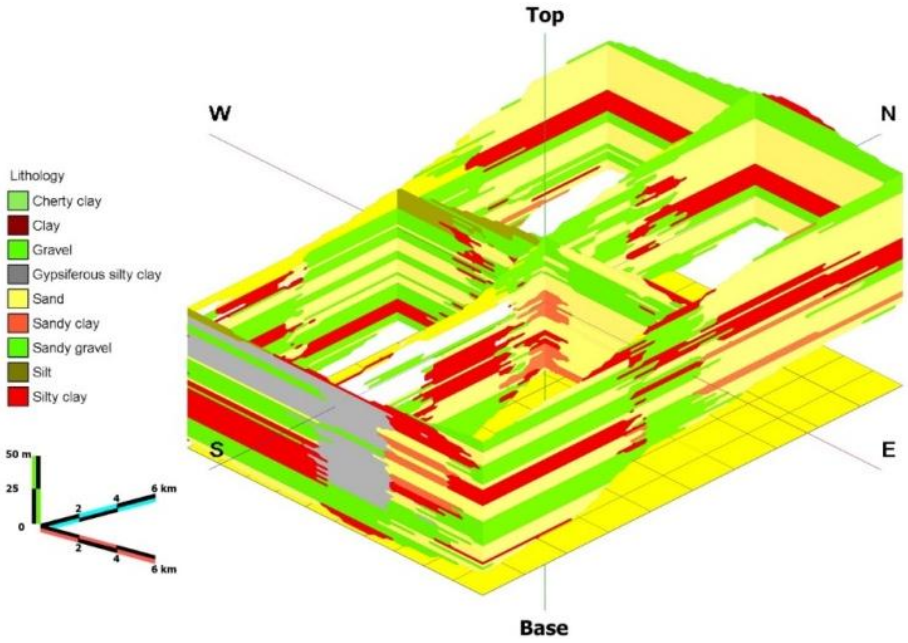

Figure 3- Fence diagram of the study area

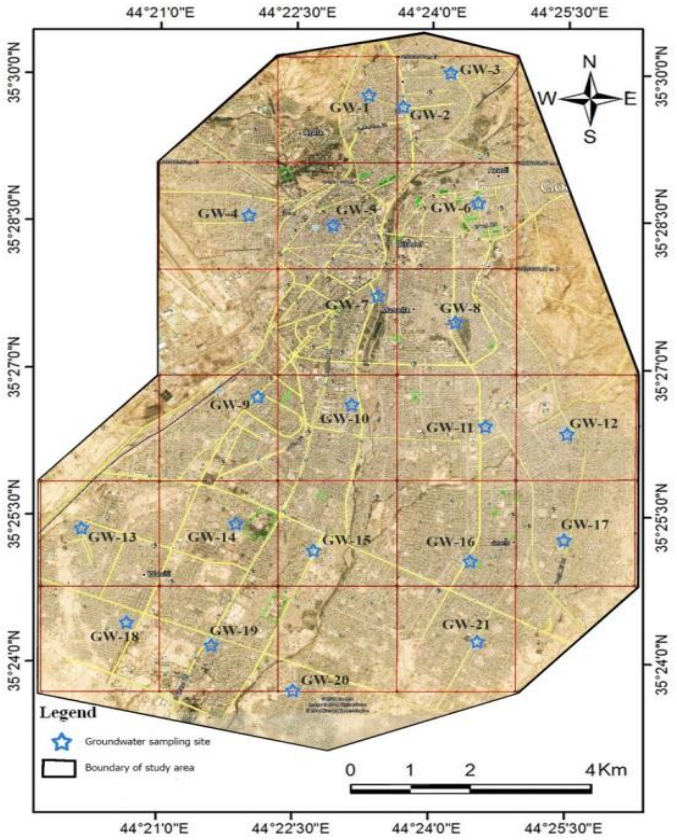

Figure 4- Loction map shows the groundwater sampling sites

Hydrogeological setting of the study area

Shallow groundwater is present in the unconfined aquifer represented by old and recent Quaternary deposits [36]. The aquifer consists of gravel, sand, silt, and clay found either as an individual layer or as a mixture with some lenses of secondary gypsum restricted in the southern part of the model area Figure-3. The groundwater occurs generally under free water-table condition. In addition to direct precipitation, groundwater bodies are fed by influent seepage from the Khassa River that runs through the city, creating beyond the north-east boundary of the aquifer. The most intensive recharge occurs on the south-west slope of the Kirkuk mountain ridge. Moreover, seepage from green spaces that found within residential and local agricultural area was another recharge sources. The thickness of the unconfined aquifers varies from 10 to 60 m Figure-4. The water table depth from land surface ranges from 1.17 to 30.95 m in dry season, whereas during wet season ranges from 0.5 to 2.23 m. The direction of groundwater flow was obtained by using measured water levels to construct flow net map, where the general direction of groundwater flow is from the high topography in the northeast part towards the lower topography in the south-west Figure-5. The average hydraulic gradient in the study area is about 8.56 m/km, and transmissivity ranges from 1728 to 10368 m^2/day. The higher values 1728 m^2/day is found near the river, and the transmissivity values decrease away from the center towards the margins. In unconfined aquifers, Storativity is similar to the specific yield of the aquifer. The storativity coefficient is in the range of 0.19 - 0.235. The low value of storativity may be as a result of the presence of clay lenses in alternation with aquifer rocks.

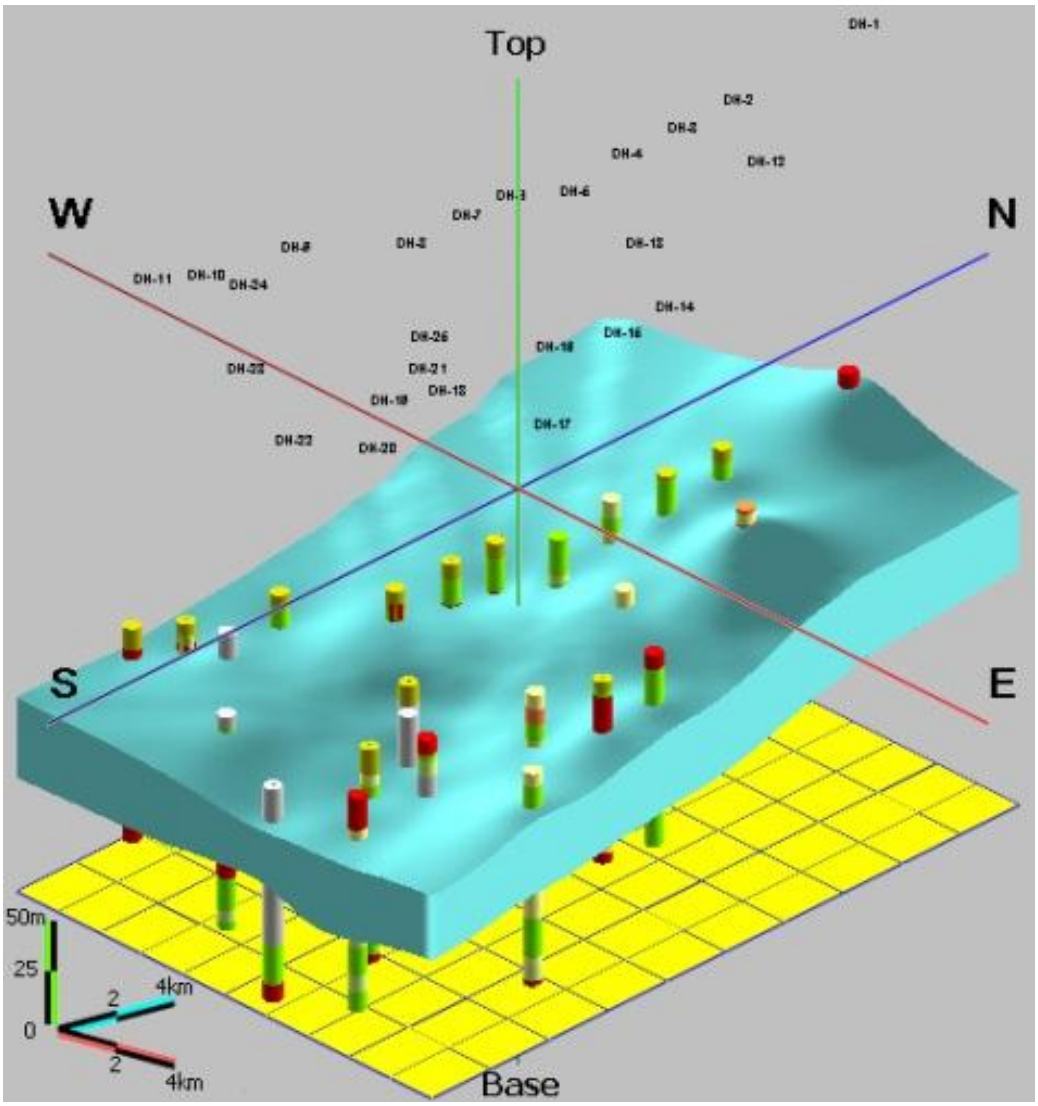

Figure 4- 3D view for the groundwater aquifer of the study area

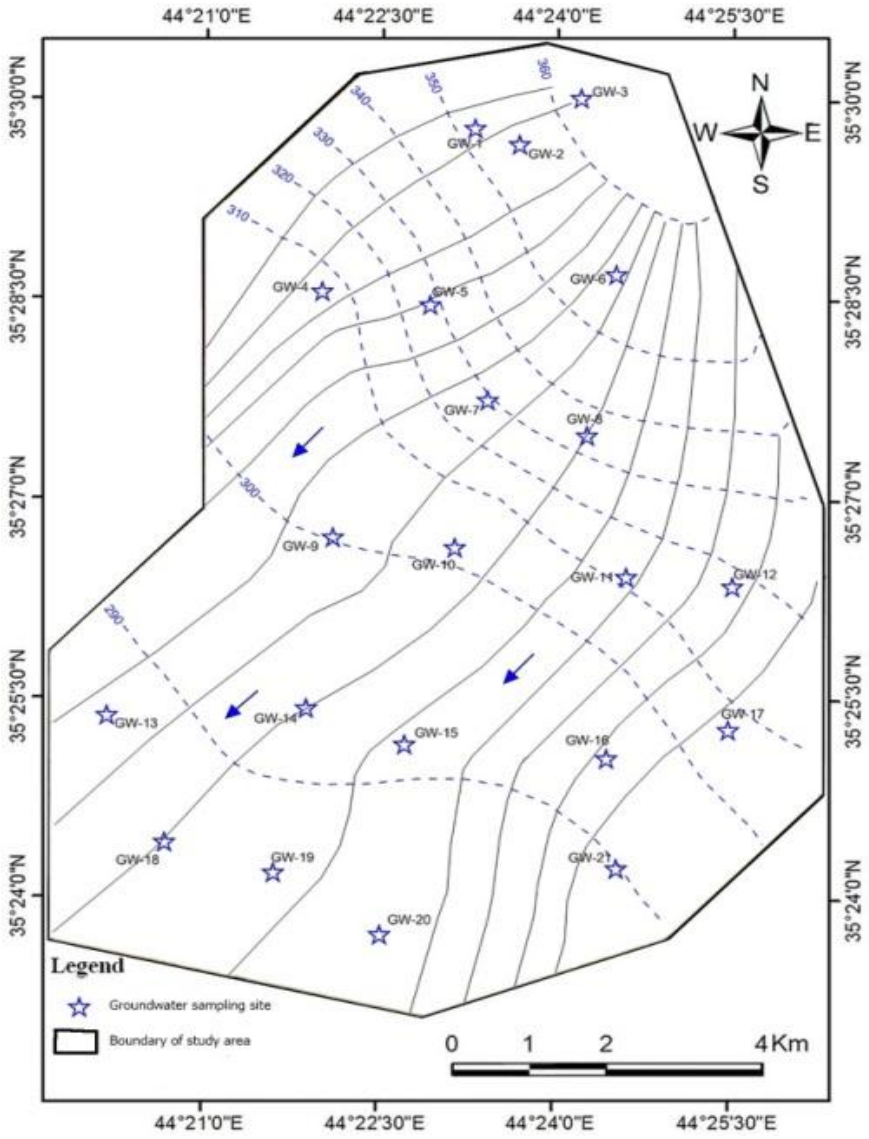

Figure 5- Flow net map of the study area

Results and discussion

Groundwater chemistry

Hydrochemical parameters are listed in Table-1, in which the highest TDS value (3856 mg/L) associated with the highest heavy metal concentrations (10 µg/L Pb, 5.32 µg/L Co, 18.4 µg/L Ni and 1258 µg/L Zn) restricted in the well GW8 as shown in the Figure-6. The high TDS value observed in the southeastern part of the city may be an indication of contamination by the area (Panja Ali) that was previously using for industrial sector. The high concentration of sulfate showed in the most water samples were ranged from 275.4 - 3050 (mg/L) in the wet season and varied from 474.6-3121 (mg/L) in dry season. The elevated Calcium concentrations with sulfate reflect the presence of secondary gypsum in soil constituent. The high chloride concentration in well GW8 indicates that local agricultural area were irrigated with sewage water. The same finding was obtained by Gvirtzman et al. [37]. The concentrations of NO_3^- (107.5-96.5 mg/L) and Na (260.7-385.5 mg/L) were also relatively high in well GW8. The high values of Na and NO3 in addition to Cl reflect that groundwater polluted by infiltrated sewage from septic tanks of surrounding residential area [38-42]. The high values of chloride (303.7- 497 mg/L) and sulfate (2010.8-2142 mg/L) in groundwater at well GW8 were clear evidence of urbanization. There are many researchers proved this fact [43, 44, 38]. The pH of an existing well GW8 (6.2–7.4) close to polluted area tend to be lower than the southwestern wells of the model area with flow direction (6.9–7.8). The relatively high groundwater pH is maybe due to high Ca. It is clear from the mentioned above that the well GW8 as the source of pollution is the most suitable site for constructing transport model as a result of the impact ancient area (Musala) in Kirkuk

city on groundwater quality from many sources, such as the seepage from adjacent local agricultural area, domestic wastewater and sewage originated from residential surrounding sites.

Table 1- Range and mean values of the hydrochemical parameters for both seasons in the studied area.

Parameters	Wet season			Dry season		
	min	max	mean	min	max	mean
Temp (˚C)	19.2	25	22.8	20	25.6	23.7
TDS (mg/L)	333	3856	1655	645	3579	1731
EC (µs/cm)	545	4820	2456	1041	4530	2613
pH	6.77	7.43	6.99	6.83	7.34	7.03
Ca (mg/L)	54.5	613.4	283.7	122.6	656.1	301
Mg (mg/L)	10.5	421.8	134.2	39.7	428.3	138.2
Na (mg/L)	19.1	418.4	129.6	41.9	634.1	160.3
K (mg/L)	1.8	16.54	6.03	1.84	16.79	5.83
HCO3 (mg/L)	49	450	164.2	15	268	101.3
SO4 (mg/L)	275.4	3050	1320.3	474.6	3121	1359.6
Cl (mg/L)	10.9	303.7	83.4	39.6	610.5	123.7
NO3 (mg/L)	7.2	208	69.67	7.25	202	67.01
NH4 (mg/L)	0.53	2.46	1.15	0.62	10.7	3.18
DO (mg/L)	1.14	8.48	3.87	1.1	8.89	4.17
Si (mg/L)	3.29	11.66	9.44	9.67	15.65	12.58
Co (µg/L)	0.08	5.32	0.54	3.34	8.85	4.75
Ni (µg/L)	2.79	18.39	5.71	2.69	13.72	4.76
Pb (µg/L)	7.88	12.31	10.25	0.43	0.86	0.62
Zn (µg/L)	6.41	1258	105.92	3.28	671.7	60.44

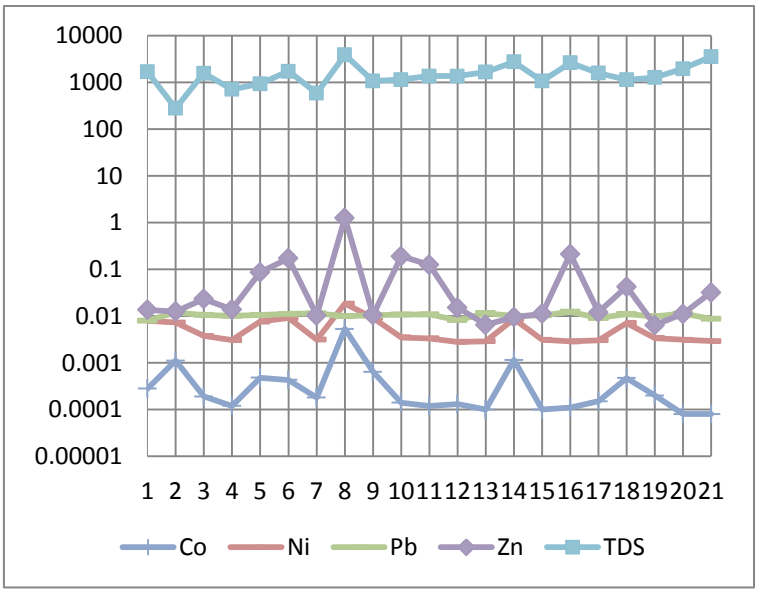

Figure 6- Comparing TDS and heavy metals values (mg/L) among groundwater samples in the study area.

Model Description:

Invers Modeling

The inverse-modeling is capable to recognize the chemical reaction that influence on groundwater quality along a flow path by calculating the moles of minerals and gases that enter or leave solution depending on the differences in their composition [22]. In the current study, the inverse-modeling is used to predict mineral phases responsible for removal of heavy metals from groundwater, whether by ion exchange or by surface complexes, to be used later in the transport-modeling as an equilibrium phase. The pathway of invers modeling was extended from the polluted site (well GW8) at the recharge region in the NE to the discharge region in the SW of study area (well GW18). GW8 and GW18 were considered as the initial and final solution respectively. The reactant phases were derived from mineralogical (XRD) tests in alluvial sediment from Majeed [45] and Al-kilabi [46] including Quartz, Plgeoclase, Calcite, Gypsum, Dolomite, Kaolinite, Illite, Montmorilinite and Palygorsckite.

Ferrihydrite [$Fe(OH)_3(a)$] was also added to determine the saturation state. Cl was added as a mole-balance control in inverse modeling. The uncertainty limits was 0.04 for initial solution (GW8) and 0.02 for final solution. The result in Table-2 show three different types of models including mole transfer of phases, in which dissolution and precipitation were noted by positive and negative values respectively. In model III, The addition of plagioclase, calcite, gypsum, kaolinite, palygorskite and illite in groundwater with flow path is further calibrated with the XRD data. Modeling results show that quartz, kaolinite, calcite, palygorskite, gypsum, plagioclase and illite were dissolving with mole transfers of 232, 189, 54.9, 20.3, 0.006, 0.0034 and 3.28E-06, respectively along the particular flow line, whereas Ca-montmorillonite, dolomite, and ferrihydrite were precipitating with mole transfers of 166.3, 27.4, and 4.88, respectively. Model III show that the fluid was under saturated with respect to Calcite and was not strongly oversaturated with respect to dolomite in comparison with ferrihydrite, indicating that the significant heavy-metal removing by precipitating carbonate phases is unlikely [47]. On the other hand, it reflects the possibility of heavy metal sorption by ferrihydrite, because of its very high surface area and amorphous structure in natural environments and able to form surface coatings on clay-size minerals in aqueous sediments [48, 49]. This result is reliable with the results of many researchers who found that most relatively low heavy-metal concentrations is surface complexation onto ferrihydrite, which appear to be the principal controls on metal sorption in fresh-water sediments [26, 50-52].

Table 2- Inverse modeling results

Phases	Model-I	Model-II	Model-III
Quartz	0.00E+00	4.06E+01	2.32E+02
$Fe(OH)_3(a)$	1.03E+00	0.00E+00	-4.88E+00
Calcite	7.84E-01	1.02E+01	5.49E+01
Gypsum	6.04E-03	6.04E-03	6.04E-03
Plagioclase	3.38E-03	3.38E-03	3.38E-03
Dolomite	-3.92E-01	-5.12E+00	-2.74E+01
Chlorite14A	1.24E+00	1.02E+00	0.00E+00
Kaolinite	2.55E+00	3.51E+01	1.89E+02
Illite	0.00E+00	0.00E+00	3.28E-06
Montmorillonite-Ca	-2.41E+00	-3.11E+01	-1.66E+02
Palygorskite	-4.30E+00	0.00E+00	2.03E+01
$O_2(g)$	-3.03E-04	-3.03E-04	-3.03E-04

Groundwater flow model

The flow and transport input file for PHAST after geometry of Kirkuk aquifer were created using ModelMuse program, which is a graphical user interface for MODFLOW and PHAST models [53]. The Kirkuk model grid extend N–S. The flow direction is NE-SW, has a horizontal extension of 13 km and a height of 230 m. The distance between nodes is 200 m in the horizontal directions and 5 m in the vertical direction. The boundary condition representing by free surface was used to define the presence of water-table and unconfined flow conditions. Ephemeral river (Khassa) was not included as a boundary condition, because it was not strongly affected on ground water level showing in flow net map Figure-5. The average Hydraulic conductivity in the study area was about 4.8 $x10^{-5}$ m/sec adpoted from Saud [54]. Steady-flow velocities is calculated by time stepping with the finite-difference flow equations that cause changes in head and flow balance within specified tolerances [55]. These velocities were used later in the transport equations throughout the simulation. Figure-7 shows that the highest velocities cover the central part of the city, where the recharge of polluted site (GW-8) causes elevating in groundwater level in about 10 m, that could be due to the urbanization that create new sources of water for recharge [56], such as leaking water mains, sewers, septic tanks and irrigated local agricultural area. These contributions not only enhance groundwater velocity but also increase their heavy metal content. These results are supported by Leung and Jiao [57] and Ocheri et al. [58].

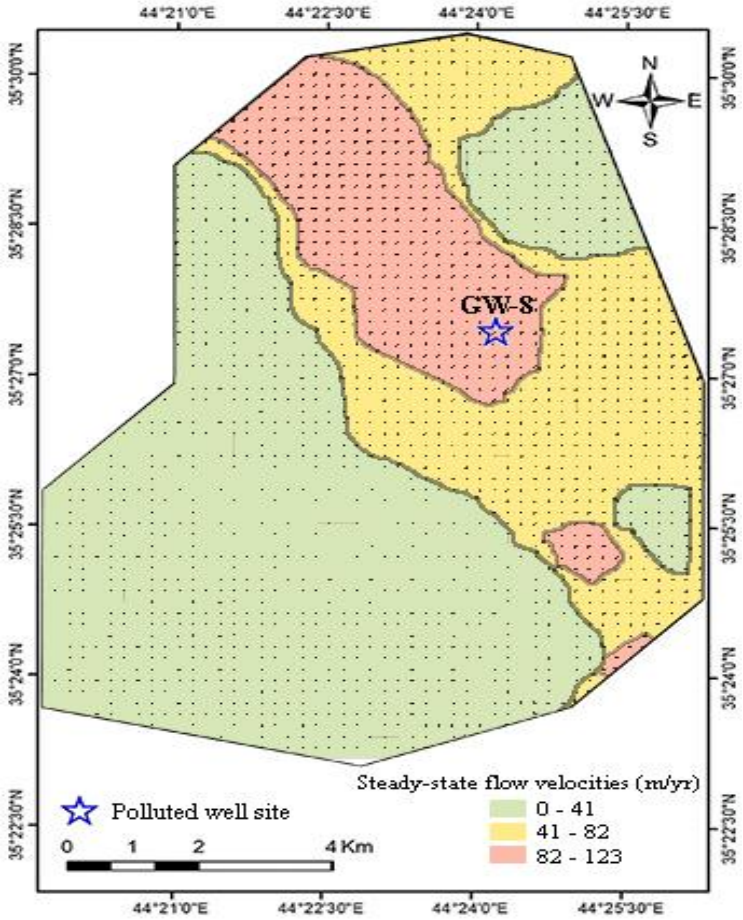

Figure 7- distribution of steady-state flow velocities

The model of the steady state flow was calibrated by correlating between simulated against observed hydraulic head [59]. Figure-8 shows often the calibration model simulate the head slightly lower than the observed head this may be due to model boundary effect [60]. However, the R^2 of simulated against observed hydraulic head is high (0.92).

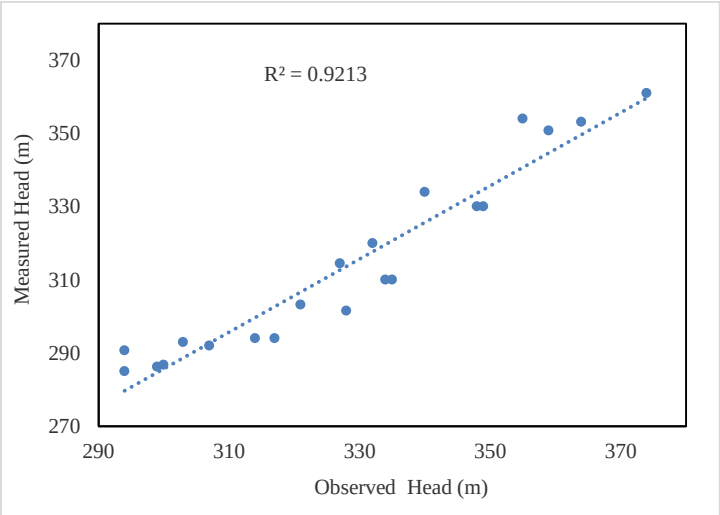

Figure 8- Scatter plot of the calibration

Reactive-transport groundwater model

The results of inverse geochemical modeling were used to determine the suitable phases for modeling of reactive transport. The groundwater flow and hydrochemical models are combined to a reactive-transport model performed using PHAST program. Effective porosity (0.22) and specific storage (0.001) were not measured but are adopted from the literatures [61-64] based on lithological

description of the studied wells. Longitudinal dispersivity (72m) was estimated based on scale-depending empirical methods of Neuman [65] and Gelhar [66] in the equations 1 and 2 respectively:

$$\alpha_x = 0.32\, L^{0.83} \quad (1)$$

$$\alpha_x = 0.1\, L \quad (2)$$

where α_x is Longitudinal dispersivity; L is the average travel distance of the plume. α_x values for equation 1 and 2 were listed in Table-3.

Table 3- Calculation Longitudinal dispersivity by the average distance of metals plume in the study area depending on Neuman [65] and Gelhar [66] equations

Metals	L (m)	αx =0.32 L^0.83 (Neuman 1990)	αx = 0.1 * L (Gelhar et al., 1992)
Co	688	73	69
Ni	969	96	97
Pb	719	75	72
Zn	438	50	44
Average		73	70

The horizontal dispersivity and vertical dispersivity were equal to 10% of the longitudinal dispersivity depending on the default percentage of ModelMuse code. The migration of the selected heavy metals was simulated using the transport model HST3D. The transport simulation was based on selected heavy metal (Co, Ni, Pb, and Zn) concentrations for polluted well (GW-8) sampled in April 2014. This is modelled with PHREEQC 2.12 on the basis of the double-layer theory of Dzombak and Morel [67]. The Model is assumed that metal-cation (M^{2+}) is the only metal species that sorbs on HFO, because the capacity for surface complexation of many toxic metals can be proved by hydrous ferric oxides [67]. the surface-complexation constants for metals were listed in Table-4.

Table 4- Surface-complexation constants for metal-cation (M^{2+}) sorption on ferrihydrite from double- Layer sorption model [67]

Cation	$\log K_1^{int}$	$\log K_2^{int}$
Co^{2+}	-0.46	-3.01
Ni^{2+}	0.37	-2.5
Pb^{2+}	4.65	0.3
Zn^{2+}	0.99	-1.99
$Hfo\_sOH^0 + M^{2+} = Fe^sOM^+ + H^+$ K_1		
$Hfo\_wOH^0 + M^{2+} = Fe^wOM^+ + H^+$ K_2		

The adsorption of a metal ion on a HFO surface involves the formation of bonds of the metal ion with the surface oxygen atoms and the release of protons from the surface (Equation 3):

$$\equiv Hfo\_OH + M^{2+} \rightarrow \equiv Hfo\_OM^+ + H^+ \quad (3)$$

where M^{2+} represents a divalent cation metal and Hfo_OH represents a hydrous ferric oxide surface. Complexation was demonstrated using the two site diffusive double layer model for HFO [67] including a strong binding site, Hfo_s, and a weak binding site, Hfo_w. The number of sites in moles of sites/L of water was entered based on Dzombak and Morel [67]. 0.2 mol weak sites and 0.005 mol strong sites per mol Fe, a surface area of 600 m2/mol Fe were used to be consistent with model for freshly precipitated Fe(OH)3(a). The amount of HFO in contact with 1 L of water was 89 g. The value of 89 is molecular weight of HFO with composition of goethite (FeOOH) [68]. In the current study, the grams of ferrihydrite were reduced to 0.089 (1000X), therefore the number of sites must be reduced proportionally to keep the applicability of the Dzomback and Morel model, because the relative number of strong and weak sites should remain constant when the total number of sites varies [69]. The transport model parameters with surface-complexation properties were listed in Table-5.

Table 5- Properties of hydrous ferric oxide used in the extraction of surface-complexation constants using Two-Layer surface-complexation model (data from Dzombak and Morel [67] with model parameters

Model Parameter	**Value**
Sorption parameters	**Value**
Specific Surface Area	600 m^2/g
High-Affinity Site Density	5E-6 moles sites / mole Fe
Low-Affinity Site Density	2E-4 moles sites / mole Fe
Mass of solid for calculation of surface area	0.089 mg HFO/ mole Fe
Point of Zero Charge	8.1
Advection model parameters	**Value**
method of calculating advection	upstream finite difference method
Dispersion model parameters	**Value (m)**
longitudinal dispersivity	72
horezontal dispersivity	7
vertical dispersivity	7
Flow model parameters	**Value**
Hydrolic conductivity	0.000048 m/sec
Effective porosity	0.22
Specific storage	0.001 m-1
Time parameters	**Value (year)**
length of simulation periods	20
time step	1

Result and Discussions

Analytical data for polluted site composition were inputted to Phreeqc. Based on invers modeling results, only one solid phase, ferrihydrite, is allowed to precipitate in the simulations because it is oversaturated comparing with other phases and it is the most likely solid to control metal solubility during the simulation time (20 years). The simulation shows that the contaminant plume with a lateral spread originating from the polluted site of local agricultural area in the central part of the city and advances towards south western part of the city a cross the Khassa stream Figure-9. Selected results of the reactive transport model in 2-D cross-sectional area 5 Km and 110 m thick with 2-D top view 4 Km width oriented in the direction of groundwater flow are shown in Figures-10, 11, and 12. Despite presence of dissolved oxygen, sulfate, and nitrate in the upstream of polluted site, the model predicts that a little proportion of weak sorption sites on HFO are occupied by sulfate ions. This result corresponds with the fact that at pH greater than or equal to 6.0, sulfate forms only outer-sphere surface complexes on HFO, whereas at pH less than 6.0 both outer- and inner-sphere surface complexes are formed on HFO surface [70-72]. For this reason the concentration of SO_4 in the pumping well (GW8) is already high, because at neutral condition, SO4 is more mobile and not sorbed on strong surface site of HFO. On the other hand, the heavy metals, as free cations, were quickly scavenged from solution near their source. The end of dissolved Co, Ni, Pb, Zn, plumes are located at about 688, 969, 719, 438 m respectively from the polluted source. The different behavior between cation and anion form arise from the fact that the surface charge of HFO becomes more negative at higher pH values, causing attraction of cations and repulsion of anions [73]. Figures-10 show the development of precipitation scavenging over 20 years with a constant source by HFO that take place at relatively neutral pH values ranged from 6.8 to 6.9. As a result of sorption reactions, hydroxyl (OH-) functional group are consumed forming hydrolysis of water molecules at the mineral surface, whereas H+ ions as protons are released [48]. These changes contribute to decrease pH value, but the dissolution of calcite along specified flow path keep the pH value approximately constant and increase the extent that pH is buffered. Consequently, the capacity of natural attenuation may enhance especially when sorpative sites (HFO) is available in aquifer materials. The same result was proved by other researchers [19,74].

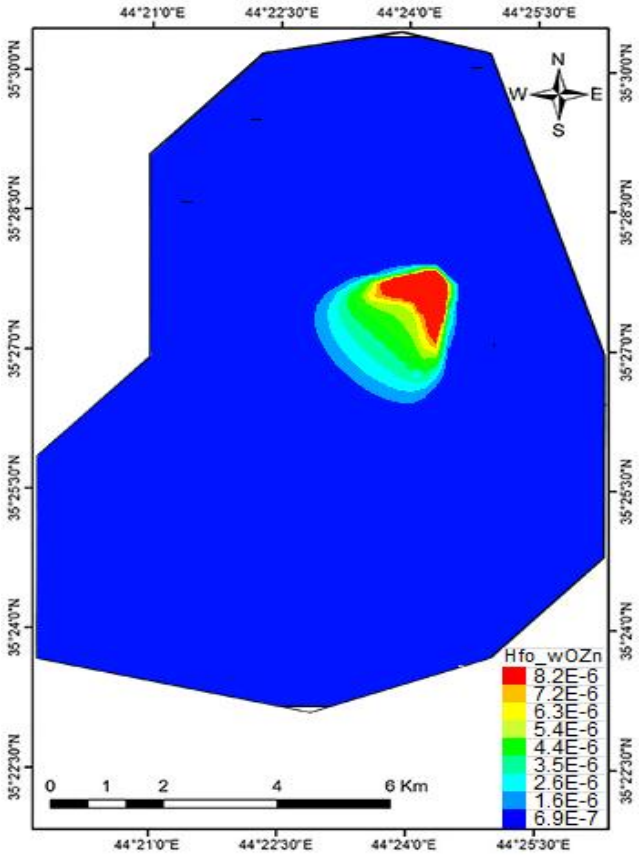

Figure 9- Location of Zn plume (mol/L) that adsorbed on weak binding site of HFO in the study area

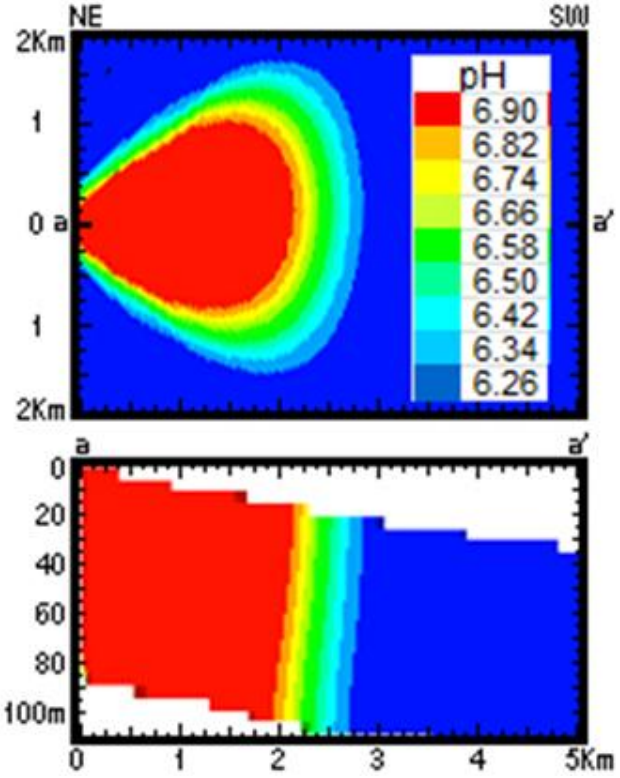

Figure 10- pH plum

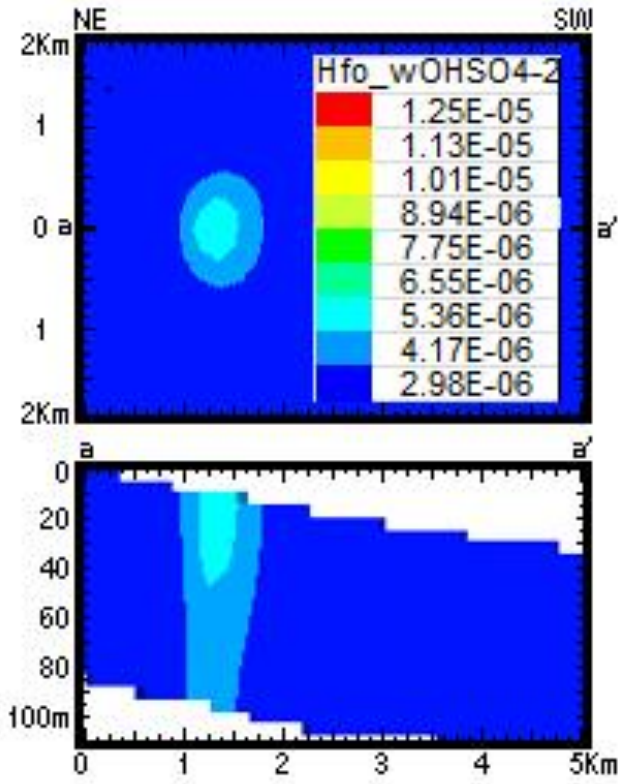

Figure 11- Sorbed SO_4^{2-} plume (mol/L) on outer-sphere of HFO

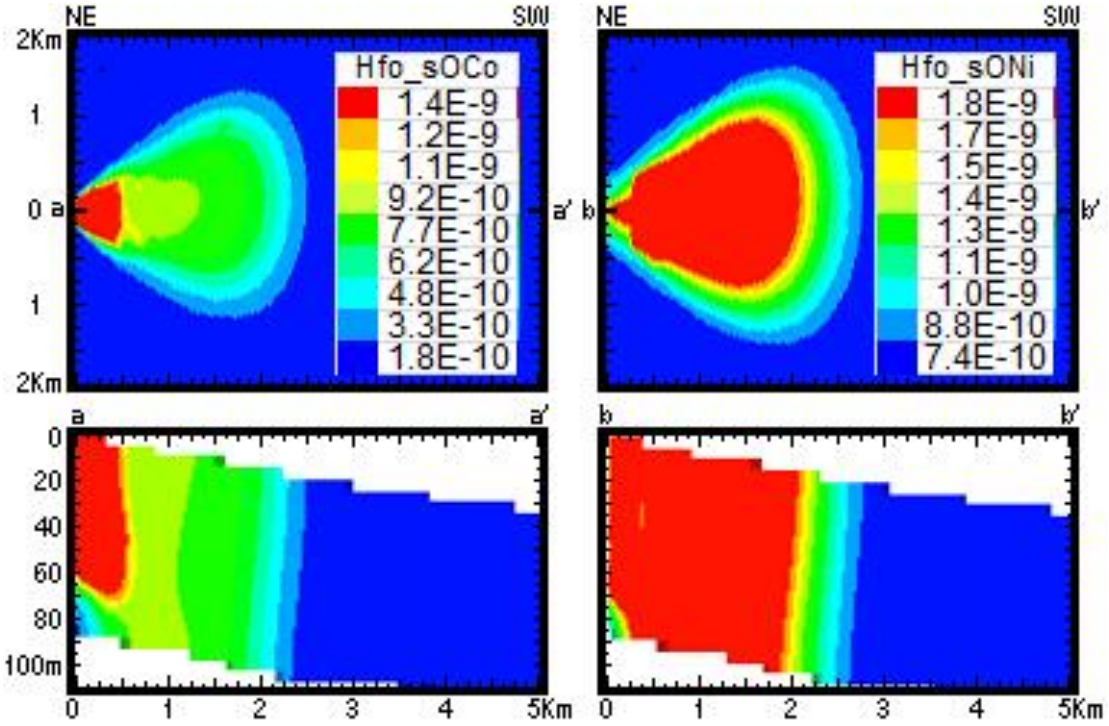

Figure 12- Sorbed Co and Ni plumes (mol/L) on strong surface sites of HFO

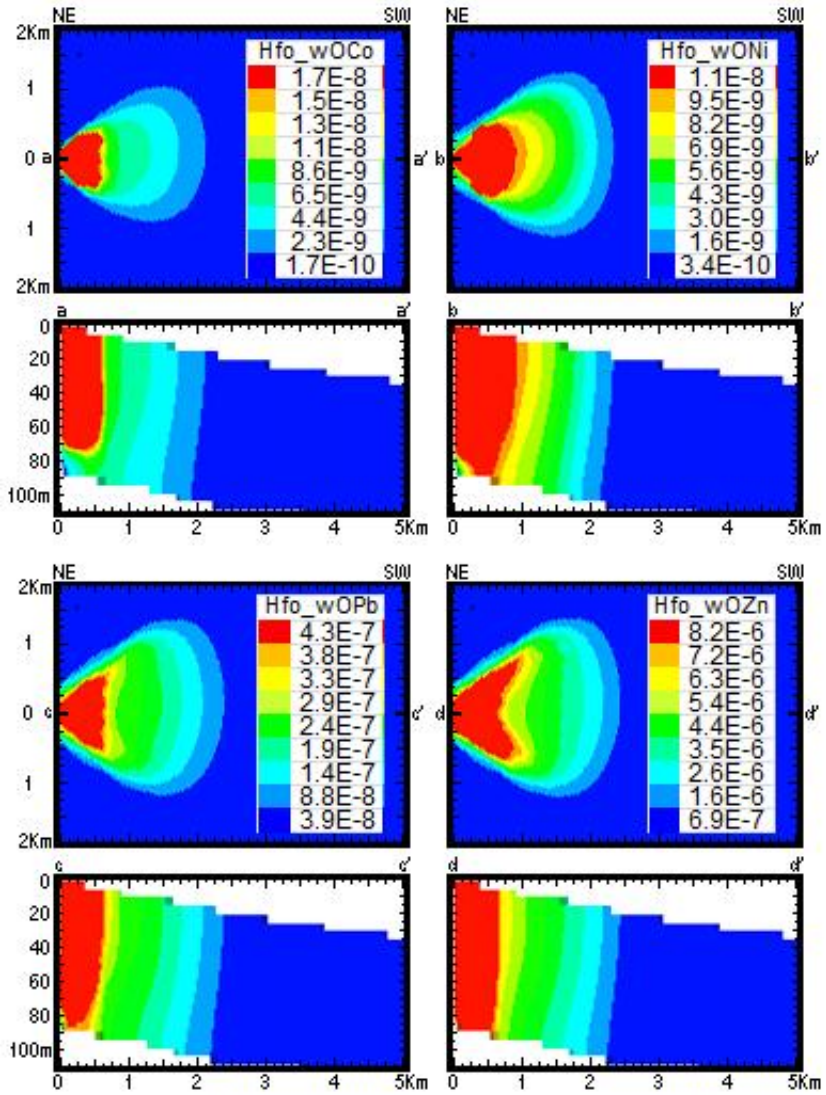

Figure 13- Sorbed Co, Ni, Pb and Zn plumes (mol/L) on weak binding site on HFO

Figures-12 and 13 show that the sorption of Pb and Zn occur only on weak binding site on hydrous ferric oxide, whereas Co and Ni pound to both outer- and inner-sphere surface complexes on HFO, because Co favorite specific sorption on ferrihydrite surface and exist at low concentration and at pH values above 5 [75]. Moreover, Cobalt considers as a retarded for the transformation of amorphous ferrihydrite to more crystalline oxides essentially by stabilizing ferrihydrite against dissolution [76]. This result is corresponding with Cornell and Giovanoli [77]. Ni is also pound to weak and strong surface complexes site, where Li and Zhang [78] proved that the main processes for nickel (II) removal is the adsorption directly on the surface of zero-valent iron. Figures-12 and 13 show that weak binding sites are sorbing more concentration of Co and Ni than strong binding site. The depletion of ferrihydrite in the study area was started at about 600 m from polluted site. The depletion may reduce the capability of HFO to scavenge heavy metal from groundwater, because HFO is thermodynamically meta-stable and initially precipitates in amorphous form [$Fe(OH)_3$(am)] in neutral to alkaline conditions, with a strong capacity to adsorb heavy metals. With time, HFO crystallize toward more stable member of the group like goethite (FeOOH), during that they lose surface area, reduce adsorption capacity, and tend to desorb heavy metals [48,79,80]. The ratios of sorbed Co, Ni, Pb and Zn concentrations to dissolved concentrations were about 21%, 31%, 100%, and 91% at pH value of 6.9, these percentages decrease to 0.4%, 3%, 9%, and 8% respectively with decrease pH value to 6.3. This result is consistent with the results of Filipek et al. [81] who found that the ratios of sorbed metals concentrations to dissolved concentrations are a function of pH with the least amount of sorption occurring at lower pH. Figures- 6.17 show that the sorption of metals is increasing, when the pH is increasing. 50 % of Ni, Zn, Pb and Co have been sorbed at the pH of 6.84 6.85, 6.86, 6.87 with

distance about 719, 1125, 1313 and 1594 m respectively from polluted site, indicating that the faster sorption of metals on hydrous ferric oxide in study area was in order Co> Pb> Zn> Ni.

Conclusion

The main contribution in natural attenuation of heavy metals in groundwater was sorption processes, which led to remove selected heavy metals, namely Co(II), Ni(II), Pb(II) and Zn(II) by ferrihydrite. The dominant processes in the Kirkuk aquifer are dissolution of calcite and precipitation of ferric hydroxides. Complexation modelling showed two type of complexes, one type associated with a weak site (Hfo_wOCo^+, Hfo_wONi^+, Hfo_wOPb^+, Hfo_wOZn^+) and the other associated with a strong site (Hfo_sOCo^+, Hfo_sONi^+) formed for all metals studied. Maximum sorption of metals was occurring through distance less than 1Km from upstream, in which can be estimated that almost all concentration of metals are scavenged by sorption. In the study area, the capacity of natural attenuation increase with increase the extent that pH is buffered by dissolution of calcite along flow path, where 50% of metals can be removed at pH range 6.9 - 6.8. For this reason, the dissolution of calcite in groundwater can have a positive influence on the attenuation of metals. The competition effects for combined metals are shown that the affinity sequence of metals for the hydrous ferric oxide in the study area was in order Co> Pb> Zn> Ni.

Acknowledgments

We thank Wael Kanoua, Alirreza Arab and one anonymous reviewer for their constructive comments. This study was supported by the Ministry of Higher Education and Scientific Research of Iraq. We are indebted to Petroleum Engineering Department/Chemical and Petroleum Engineering Faculty/Homs/Syria for support in preparation of the performing the simulations for the model.

References:

1. Robertson, W.D., Cherry, J.A. and Sudicky, E.A. **1991**. Ground-water contamination from two small septic systems on sand aquifers. *Ground Water*, 29 (1), pp:82–92.
2. Jeong, C.H. **2001**. Effect of land use and urbanization on hydrochemistry and contamination of groundwater from Taejon area, Korea. *Journal of Hydrology*, 253, pp:194–210.
3. Rivett, M.O., Petts, J., Butler, B. and Martin, I. **2002**. Remediation of contaminated land and groundwater: experience in England and Wales. *Journal of Environmental Management*, 65, pp; 251–268.
4. Dechesne, M., Barraud, S., and Bardin, J. P. **2004**. Indicators for hydraulic pollution retention assessment of stormwater infiltration basins. *Journal of Environmental Management*, 71, pp:371–380.
5. Chidambaram, S., Anandhan, P., Prasanna, M. V., Ramanathan, AL., Srinivasamoorthy K., and Kumar, G. **2012**. Hydrogeochemical Modelling for Groundwater in Neyveli Aquifer, Tamil Nadu, India, Using PHREEQC: A Case Study. *Natural Resources Research*, 21(3), pp: 311-324.
6. Custodio, E. **1997**. Groundwater quantity and quality changes related to land and water management around urban areas: blessing and misfortunes. *Groundwater in the Urban Environment. Problems, Processes and Management*, 1, pp: 11-22.
7. Vidal, M., Melgar, J., Lo´ pez, A., Santoalla, M.C. **2000**. Spatial and temporal hydrochemical changes in groundwater under the contaminating effects of fertilizers and wastewater. *Journal of Environmental Management*, 60, pp:215–225.
8. Ottesen, R.T., Langedal, M. **2001**. Urban geochemistry in Trondheim, Norway. *NGU-BULLETIN*, 438, pp:63–69.
9. Grzebisz, W., Ciesla, L., Komisarek, J., Potarzycki, J. **2002**. Geochemical assessment of heavy metals pollution of urban soils. *Polish J. Environ. Stud*. 11(5), pp: 493–499.
10. Wong, S.C., Li, X., Thornton, I. **2006**. Urban environmental geochemistry of trace metals, *Environmental Pollution*, 142, pp:1-16.
11. Mohrlok, U. and Schiedek, T. **2007**. Urban impact on soils and groundwater – From infiltration processes to integrated urban water management. *JSS - J Soils & Sediments*, 7 (2), p:68.
12. Boschetti, T., Falasca, A., Bucci, A., De Felice, V., Naclerio, G. and Celico, F. **2014**. Influence of soil on groundwater geochemistry in a carbonate aquifer, southern Italy. *International Journal of Speleology*, 43 (1), pp:79-94. Tampa, FL (USA) ISSN 0392-6672 http://dx.doi.org/10.5038/1827-806X.43.1.8.
13. Mohammed, F.A. **2009**. Pollution Caused by Vehicle Exhausts and Oil Trash Burning in Kirkuk city. *Iraqi Journal of Earth Sciences*, 9 (2), pp: 39-48.

14. Kanbour, F.I., Kitto, A.M.N., Yassein, S., AI-Taie F.A. and Ali, A. **1985**. Elemental analysis of total suspended particulate matter in the ambient air of Baghdad. *Envir. Int.* 11, pp:459-463.

15. Ismail, S. A. **2004**. Atmospheric pollution and environmental effect in Kirkuk area, Iraq. 6th intern. Conf. On Geochemistry, Alex. Univ., Egypt, I5-16, pp:23-28.

16. Ali, L.A. **2013**. Environmental Impact Assessment Of Kirkuk Oil Refinery, Ph.D., Thesis, University of Baghdad, p:217.

17. Mustafa, S.S., Mustafa, S.S., Mutlag, A.H. **2013**. Kirkuk municipal waste to electrical energy, *Electrical Power and Energy Systems*, 44, pp:506–513.

18. Tedeschi, S. **1990**. Surface and groundwater use in the urban area of Zagreb, Hydrological Processes and Water Management in Urban Areas (Proceedings of the Duisberg Symposium, April 1988). IAHS Publ. no. 198, pp:95-99.

19. Ford, R.G., Wilkin, R.T. and Puls, R.W. **2007**. Monitored Natural Attenuation of Inorganic Contaminants in Ground Water – Volume 2, Assessment for Non-Radionuclides Including Arsenic, Cadmium, Chromium, Copper, Lead, Nickel, Nitrate, Perchlorate, and Selenium. *U.S. Environmental Protection Agency*, 600(R), pp: 17-40.

20. Kipp, K.L. **1987**. HST3D—A computer code for simulation of heat and solute transport in three-dimensional ground-water flow systems. USGS Water-Resources Investigations Report 86–4095.

21. Kipp, K.L. **1997**. Guide to the revised heat and solute transport simulator HST3D—Version 2. USGS Water-Resources Investigations Report 97–4157.

22. Parkhurst, D.L. and Appelo, C.A.J. **1999**. User's guide to PHREEQC (version 2): A computer program for speciation, batch-reaction, one-dimensional transport, and inverse geochemical calculations: U.S. Geological Survey Water-Resources Investigations Report 99-4259, p:312.

23. Parkhurst, D. **2002**. "Selective Attention in Natural Vision: Using Computational Models to Quantify Stimulus-Driven Attentional Allocation. Unpublished Ph.D. Thesis, Johns Hopkins University, Baltimore, MD.

24. Charlton, S.R., and Parkhurst, D.L. **2012**. Phast4Windows: A 3D graphical user interface for the reactive-transport simulator PHAST: Ground Water, in press, U.S. Geological Survey, p:14.

25. Schippers, J.C., Petrusevski, B., and Sharma, S.K.**2004**. *Module "Groundwater Resources and Treatment*, UNESCO-IHE Institute for Water Education, The Netherlands, p:166.

26. Jenne, E.A. **1968**. Controls on Mn, Fe, Co, Ni, Cu, and Zn concentrations in soils and water—the significant role of hydrous Mn and Fe oxides; in Gould, R.F. (ed.),Trace Inorganics in Water, *Advances in Chemistry Series*, 73, pp:337–387.

27. Hem, J.D. **1985**. Study and interpretation of the chemical characteristics of natural water, 3rd Edition: U.S. Geological Survey Water-Supply Paper 2254, p:263.

28. Šráček, O., Zeman, J. **2004**. *Introduction to Environmental Hydrogeochemistry*, Masaryk University, Pron, p:102.

29. Frenken, K., ed. **2009**. Irrigation in the Middle East region in figures. FAO Water Report 34. Rome: Food and Agricultural Organization of the United Nations. ftp://ftp.fao.org/docrep/fao/012/i0936e /i0936e01.pdf.

30. Buringh, P. **1960**. Soil and soil condition of Iraq, Ministry of Agriculture, Directorate General of Agriculture Research and Project, Baghdad, p:332.

31. Buday, T. **1980**. Rigional Geology of Iraq: Stratigraphy and Palegeography. State Organization of Minerals, Baghdad, p:445.

32. Kassab, I.I.M. and Jassim S.Z., **1980**. The Regional Geology of Iraq, general directorate for geological survey and mineral, Baghdad, Iraq.

33. Jassim, S.Z., Karim, S.A., Basi, M., Al-Mubarak, M.A. and Munir, J. **1984**. Final report on the regional geological survey of Iraq. Vol.3, Stratigraphy. Manuscript report, Geological Survey of Iraq.

34. Jassim, S.Z. and Goff, J.C. **2006**. Geology of Iraq, First Edition, Czech Republic, Isban, p:341.

35. De Vivo, B., Belkin, H.E. and Lima, A. **2008**. *Environmental Geochemistry*. Site Characterisation, Data Analysis and Case Histories. Amsterdam: Elsevier, pp:837–842.

36. Al-Naqash, A.B., Ismaeel, S.Kh., Hasan, A.H. and Rahi, Kh.M. **2003**. Evaluation study and setting of production program for wells of national campaign project for water well drilling in Kirkuk governorate, internal report, Ministry of irrigation , General company for water well drilling, p:185. (In Arabic)

37. Gvirtzman, H., Ronen, D., Magaritz, M., **1986**. Anion exclusion during transport through the unsaturated zone, *Journal of Hydrology*, 87, pp: 267-283

38. Eisena, C., and Anderson, M.P. **1979**. The effects of urbanization on ground-water quality: A case study: *Ground Water*, 17 (5), pp: 456–462.

39. Naftz, D.L. and Spangler, L.E. **1994**. Salinity increases in the Navajo Aquifer in southeastern Utah. *Water Resources Bulletin*, 30 (6), pp:1119-1135.

40. Eiswirth, M., and Hotzl, H. **1997**. *The Impact of Leaking Sewers on Urban Groundwater*. In: J. CHILTON (eds), Groundwater in the Urban Environment. Balkema Publications, Rotterdam, The Netherlands, pp:399 - 404.

41. Mason, C.F., Norton, S.A., Fernandez, I.J. and Katz, L.E. **1999**. Deconstruction of the chemical effects of road salt on stream water chemistry. *Journal of Environmental Quality*, 28, pp: 82-91.

42. Buttle, J.M. and Labadia, C.F. **1999**. Deicing salt accumulation and loss in highway snowbanks. *Journal of Environmental Quality*, 28, pp: 155-164.

43. Long, D.T. and Saleem, Z.A. **1974**. Hydrogeochemistry of carbonate ground waters of an urban area. *Water Resources Research*. 10(6), pp: 1229-1238.

44. Schicht, R.J. **1977**. The effect of precipitation scavenging of airborne and surface pollutants on surface and groundwater quality in urban areas. Final Report-Part 1, Groundwater studies. Illinois State Water Survey Contract Report 185.

45. Majeed, N.N., **2004**. Geotechnical study of gypseous soil chosen from places in Kirkuk city, Ph.D. Thesis, University of Baghdad, p:151 (In Arabic)

46. Al-Kilabi, J.A.H. **2013**. Hydrogeochemistry of groundwater and the probable effect of Kirkuk irrigation project on its quality in Al-Hawija area, Iraq, Ph.D. Thesis, University of Baghdad, p:178.

47. Schwartz, M.O. and Ploethner, D. **1999**. Removal of heavy metals from mine water by carbonate precipitation in the Grootfontein- Omatako canal, Namibia. *Environ Geol*, 39, pp:1117–1126.

48. Smith, K.S., **1999**. Metal sorption on mineral surfaces: an overview with examples relating to mineral deposits, Chapter 7, in Plumlee, G.S., and Logsdon, M.J., eds., The environmental geochemistry of mineral deposits, Part A: Processes, techniques, and health issues, Reviews in Economic Geology, Vol. 6A: Littleton, Colorado, Society of Economic Geologists, Inc., pp:161-182.

49. Schwertmann, U. and Cornell, R.M. **2000**. *Iron Oxides in the Laboratory*: Preparation and Characterization, 2nd edition. Wiley-VCH Verlag, Weinheim, Germany.

50. Ali, M.A. and Dzombak, D.A. **1996**. Competitive sorption of simple organic acids and sulfate on goethite. *Environ. Sci. Technol.* 30, pp: 1061-1071.

51. Swedlund, P.J. and Webster, J.G. **2001**. Cu and Zn ternary surface complex formation with SO4 on ferrihydrite and schwertmannite. *Appl. Geochem.* 16 (5), pp: 503–511.

52. Schwartz, M.O. and Kgomanyane, J. **2008**. Modelling natural attenuation of heavy-metal groundwater contamination in the Selebi-Phikwe mining area, Botswana, *Environ. Geol*., 54, pp:819–830

53. Winston, R.B. **2009**. *Model Muse: A Graphical User Interface For MODFLOW–2005 and PHAST*: U.S. Geological Survey Techniques and Methods, book 6, chap. A29, p:52.

54. Saud, Q.J. **2009**. Hydrogeological and hydrochemical study of Kirkuk governorate, Northern Iraq, Jour. *Geol. Min. Irq*., 5 (1), pp: 1-15.

55. Parkhurst, D.L., Kipp, K.L., Engesgaard, Peter, and Charlton, S.R. **2004**. PHAST: A program for simulating ground-water flow, solute transport, and multicomponent geochemical reactions: U.S. Geological Survey Techniques and Methods 6–A8, p:154.

56. Lerner, D.N. **1990**. Groundwater recharge in urban areas. Almas. *Environ*. 24B, pp:29-33

57. Leung, C.M. and Jiao J.J. **2006**. Heavy metal and trace element distributions in groundwater in natural slopes and highly urbanized spaces in Mid-Levels area, Hong Kong. *Water Research* 40(4), pp: 753-767.

58. Ocheri, M.I., Odoma, L.A. and Umar, N.D. **2014**. Groundwater quality in Nigeria urban areas: A review, Global Journal of Science Frontier Research: *H Environment & Earth Science*, 14(3), pp:35-45.

59. Anderson, M.P. and Woessner, W.W. **1992**. *Applied Groundwater Modeling. Simulation of Flow and Advective Transport*. Academic Press, San Diego. p:381.

60. Seneviratne, A.A.A.K.K. **2007**. Development of steady state groundwater flow model in lower Walawa Basin – Sri Lanka, Unpublished M.Sc. Thesis, International Institute for Geo-information and Earth Observation.
61. Domenico, P.A. and Mifflin, M.D. **1965**. Water From Low-Permeability Sediments and 632 Land Subsidence. Water Resources Research, American Geophysical Union, vol. 1,
62. Castany, G. **1967**. Introduction à l'étude des courbes de tarissement. Chronique d'hydrogéologie, pp:23-30.
63. Domenico, P.A. and Schwartz, F.W. **1990**. *Physical and Chemical Hydrogeology*. John Wiley & Sons, Inc., New York, NY.
64. Younger, P.L. **1993**. Possible Environmental Impact of the Closure of Two Collieries in County Durham. *Journal of the Institution of Water and Environmental Management*, 7, pp: 521-531.
65. Neuman, S.P. **1990**. Universal scaling of hydraulic conductivities and dispersivities in geological media. *Water Resources Research*; 26(8), pp:1749-1758.
66. Gelhar, L. W., and C. L. Axness.**1983**.Three-dimensional stochastic analysis of macrodispersion in aquifers, *Water Resour. Res.*, 19(1), pp:161–180
67. Dzombak, D.A. and Morel, F.M.M. **1990**. *Surface Complexation Modeling*. Hydrous ferric oxide. John Wiley & Sons, New York.
68. Šráček, O., Černik, M. and Vencelides, Z. **2013**. Applications of Geochemical and Reactive Transport Modeling in Hydrogeology (First Edition). Palacký University, Olomouc, Czech Republic.
69. Parkhurst, D.L. and Appelo, C.A.J. **2013**. *Description of Input and Examples for PHREEQC Version 3, A Computer Program for Speciation, Batch-Reaction, One-Dimensional Transport, and Inverse Geochemical Calculations*. U.S. Geological Survey Techniques and Methods, book 6, chap. A43, p:497.
70. Bigham, J.M., Schwertmann, U., Carlson, L. and Murad, E. **1990**. A poorly crystallized oxyhydroxysulfate of iron formed by bacterial oxidation of Fe(II) in acid mine waters. *Geochim. Cosmochim. Acta*, 54, pp: 2743-2758.
71. Peak, D., Ford, R.G. and Sparks, D.L. **1999**. An in situ ATR-FTIR investigation of sulfate bonding mechanisms on goethite. *J. Coll. Interf. Sci.* 218, pp: 289–299.
72. Peak, D. and Sparks, D.L. **2002**. Mechanisms of selenate adsorption on iron oxides and hydroxides. *Environ. Sci. Technol*. 36 (7), pp: 1460–1466.
73. Langmuir, D. **1997a**. *Aqueous environmental chemistry*. Upper Saddle River, NJ: Prentice-Hall. p:600.
74. Miotlinski, K. **2008**. Coupled reactive transport modeling of redox processes in a nitrate-polluted sandy aquifer, *Aquatic Geochemistry*, 14(2), pp:117–131.
75. Tiller, K. G., Hodgson, J. F. and Peech, M. 1963. Specific sorption of cobalt by soil clays. *Soil Sei.*, 95, pp: 392-399
76. Perez-Espinosa, A., Moral, R., Moreno-Caselles, J., Cortes, A., Perez-Murcia, M.D. and Gomez, I. **2005**. Co phytoavailability for tomato in amended calcareous soils. *Bioresource Technology*, 96, pp: 649-655.
77. Cornell, R.M. and Giovanoli, R.**1988**.The influence of copper on the transformation of ferrihydrite (5Fe2O3.9H2O) into crystalline products in alkaline media. *Polyhedron*,7, pp:385-391.
78. LI, X.–Q. and ZHANG, W. X. **2007**. Sequestration of Metal Cations with Zerovalent Iron Nanoparticles: A Study with High Resolution X–Ray Photoelectron Spectroscopy (HRXPS), *Journal of Physical Chemistry*, 111(19), pp: 6939–6946.
79. Jambor, J.L. and Dutrizac, J.E. **1998**. Occurrence and constitution of natural and synthetic ferrihydrite, a widespread iron oxyhydroxide. *Chem. Rev*., 98, pp:2549-2585
80. Langmuir, D., Chrostowski, P., Vigneault, B., Chaney, R. **2005**. Issue paper on the environmental chemistry of metals. *U. S. Environmental Protection Agency*, Risk Assessment Forum, Draft contract Report pp:1- 39.
81. Filipek, L.H., Nordstrom, D.K., and Ficklin, W.H. **1987**. Interaction of acid mine drainage with waters and sediments of West Squaw Creek in the West Shasta Mining District, California: *Environmental Science and Technology*, 21, pp: 388–396.